
q POTS: Efficient batch multiobjective Bayesian optimization via Pareto optimal Thompson sampling

Ashwin Renganathan

The Pennsylvania State University,
University Park, PA 16802

E-mail: ashwin.renganathan@psu.edu

Abstract

Classical evolutionary approaches for multi-objective optimization are quite effective but incur a lot of queries to the objectives; this can be prohibitive when objectives are expensive oracles. A sample-efficient approach to solving multiobjective optimization is via Gaussian process (GP) surrogates and Bayesian optimization (BO). Multiobjective Bayesian optimization (MOBO) involves the construction of an acquisition function which is optimized to acquire new observation candidates. This “inner” optimization can be hard due to various reasons: acquisition functions being nonconvex, nondifferentiable and/or unavailable in analytical form; the success of MOBO heavily relies on this inner optimization. We do away with this hard acquisition function optimization step and propose a simple, but effective, Thompson sampling based approach (q POTS) where new candidate(s) are chosen from the Pareto frontier of random GP posterior sample paths obtained by solving a much cheaper multiobjective optimization problem. To further improve computational tractability in higher dimensions we propose an automated active set of candidates selection combined with a Nyström approximation. Our approach applies to arbitrary GP prior assumptions and demonstrates strong empirical performance over the state of the art, both in terms of accuracy and computational efficiency, on synthetic as well as real-world experiments.

1 Introduction

Numerical optimization plays a vital role in the design of complex engineered systems. Real world engineered systems are seldom designed based on a single objective; they typically involve multiple, conflicting, objectives where, the optimal design is a careful compromise between the objectives. For instance in the design of automobiles, which are designed for fuel efficiency, safety, and agility, all of which can be conflicting. Outside of engineering, in machine learning, models must be fit for maximum accuracy with the simplest architecture possible. In this work, we consider multiobjective optimization, where we have two or more conflicting objectives. Specifically, we consider the unconstrained optimization of K objectives

$$\max_{\mathbf{x} \in \mathcal{X}} \{f_1(\mathbf{x}), \dots, f_K(\mathbf{x})\},$$

where \mathbf{x} is the design variable, \mathcal{X} is the feasible set, $\mathbf{x} \in \mathcal{X} \subset \mathbb{R}^d$, $f_i : \mathcal{X} \rightarrow \mathbb{R}$, $\forall i = 1, \dots, K$, and all f_i ’s are zeroth-order oracles. What we are interested in is finding the Pareto set \mathcal{X}^* which is the set of all points in \mathcal{X} where $f_i(\mathbf{x}^*) \geq f_i(\mathbf{x})$, $\forall \mathbf{x}^* \in \mathcal{X}^*$, $\mathbf{x} \in \mathcal{X}$ and the inequality being strict for at least one of the objectives. The f_i ’s evaluated on the Pareto set are called “nondominated”, owing to the fact that no other $\mathbf{x} \in \mathcal{X}$ can improve an objective on this set without worsening another. The objectives evaluated on the Pareto set forms the Pareto *frontier* \mathcal{Y}^* in the objective space. In practice, both \mathcal{X}^* and \mathcal{Y}^* have infinite cardinality—we only seek a finite approximation of them.

We assume that all the objectives, in addition to being zeroth-order oracles, are computationally expensive to evaluate. Therefore, we are interested in sample-efficient (that is, minimal queries to the oracles) approaches to solve our problem. Evolutionary algorithms such as the nondominated sorting genetic algorithm (NSGA-II) [14] are a popular choice for solving multiobjective problems (see [65] for a review). However,

EA based approaches are known to be not sample efficient, which could be prohibitive with expensive oracles. A common approach to solving this problem under such circumstances is to use Bayesian optimization (BO) with Gaussian process (GP) surrogate models for each objective. The idea is to fit a GP model for the objectives using some initial observations $\mathcal{D}_n^i = \{(\mathbf{x}_j, y_j), j = 1, \dots, n\}$ (where we denote $y_j = f_i(\mathbf{x}_j)$) and construct an appropriate *acquisition* function that quantifies the utility of a candidate point \mathbf{x} . Then, an inner optimization problem is solved to choose new point(s) that maximize the acquisition function. The surrogate models are updated with observations at the new points and this process is repeated until a suitable convergence criterion is met. BO is very popular in the single objective ($K = 1$) case; for instance, the expected improvement (EI) [30] and probability of improvement (PI) [37, 29], quantifies the probabilistic improvement offered by a candidate point over the “best” observed point so far. The GP upper confidence bound (UCB) [50] makes a conservative estimate of the maximum using the current GP estimate of the function. Other acquisition functions, for $K = 1$, include entropy-based [56, 25], knowledge gradient (KG) [18, 58, 59], and stepwise uncertainty reduction [39, 7].

Naturally, one is tempted to extend the ideas from single objective BO to the multiobjective setting. The EI and PI acquisition functions can be extended to the multiobjective setting via the expected hypervolume improvement (EHVI) [8, 17]; gradient based extensions of the EHVI also exists [61, 11]. Similarly, the SUR criterion extended to multiobjective problems [40] is another example. There are other approaches, that draw from single-objective BO as well. For instance, ParEGO [31] scalarizes the K objectives using randomly drawn weights, which is then treated like a single-objective using EI. MOEA/D-EGO [62] extends ParEGO to the batch setting using multiple random scalarizations and the genetic algorithm MOEA/D [64] to optimize these scalarizations in parallel. Extensions of ParEGO to the batch setting (qParEGO) and its noisy variant, qNParEGO, have also been proposed [13]. [38] do a, similar, “Chebyshev” scalarization on the objectives but use Thompson sampling (TS) instead on the scalarized objective. [63] propose to use a hypervolume scalarization with the property that the expected value of the scalarization over a specific distribution of weights is equivalent to the hypervolume indicator. The authors propose a upper confidence bound algorithm using randomly sampled weights, but provide a very limited empirical evaluation. Another approach based on TS is that of [5] where candidates from a Pareto set identified from posterior GP samples are then evaluated for maximum hypervolume improve-

ment. As we will show later on, our method is closely related to [5] but differs in several ways.

DGEMO [32] is a recent method for parallel MOBO that greedily maximizes HVI while balancing the diversity of the design points being sampled. Although DGEMO scales well to large batch sizes, it does not account for noisy observations. Pareto active learning (PAL) [66] seeks to classify each candidate point in terms of their probability of being Pareto optimal or not, depending upon the GP posterior uncertainty. This approach presents another difficult acquisition function optimization that is handled via a discretized \mathcal{X} in [66].

Recent efforts [12, 13] extend the EHVI idea to sample a batch of points ($q > 1$) for parallel evaluation and with gradient computation for efficient optimization. However, the stochasticity of the acquisition functions and the associated difficulty in their optimization, particularly as q increases, remains. The entropy based acquisition functions have also been extended to the multiobjective setting; see e.g., predictive entropy search (PESMO) [24] and max-value entropy search (MESMO) [2]. MESMO improves upon PESMO in terms of scalability and computational cost however, the acquisition function is still not available in closed form and requires sample approximations. PFES[52] propose a closed-form entropy criterion for MOBO, but they depend on Pareto frontier samples and are restricted to stationary GP kernels. Additionally, joint entropy search multiobjective optimization (JESMO) [26, 55] which considers the joint information gain for the optimal set of inputs and outputs, still depends on approximations to the acquisition function. We consider the three information theoretic acquisition functions PESMO, JESMO, and MESMO as state-of-the-art that we want to compare our approach against.

Contributions. All of these approaches have a common thread: the computation of an acquisition function and its optimization which have major limitations. Firstly, the acquisition functions might not have a closed-form expression that can be easily evaluated. Secondly, the acquisition functions might not be differentiable. Thirdly, while differentiable acquisition functions have been presented [12], they can be highly nonconvex and stochastic making optimization hard. Additionally, note that batch variants of closed-form acquisition functions might not be in closed-form. All these factors motivate us to consider an approach where we do away with constructing a probabilistic acquisition function (and its maximization). Instead, we solve cheap multiobjective optimizations on the posterior GP samples to generate candidates. It is worth mentioning that our work mirrors recent efforts on choosing acquisition candidates in BO without optimization [22].

Our central idea is inspired from TS in single-objective optimization; whereas TS selects candidate points according to the probability that they are optimal, our approach selects points according to the probability that they are Pareto optimal. Therefore, we call our method Pareto optimal Thompson sampling or q POTS, where the q stands for "batch" acquisition. A very useful consequence of our approach is that selecting a batch of q points (for parallel evaluation) is simply sub-sampling from the Pareto set of our multiobjective optimization subproblems.

The rationale behind our approach is as follows. Under low posterior uncertainty, the random Pareto frontier is likely a good approximation of \mathcal{Y}^* , and thus we can exploit. On the other hand, under high posterior uncertainty, the random Pareto frontier is likely far from \mathcal{Y}^* and thus we can explore. Therefore our approach is endowed with a natural balance between exploration and exploitation. As previously stated, our approach appears similar to [5] but is significantly different. Firstly, our method circumvents the hypervolume (see Section 2.2 for a definition) computation part, which scales exponentially with the number of objectives. Secondly, batch acquisition in [5] becomes intractable with batch size; in contrast, batch acquisition in our approach comes at the *same* cost as sequential acquisitions. Finally, since we don't use random Fourier features [41] as in [5], our approach applies more widely to include nonstationary GP kernels such as deep GPs [10, 4, 46, 42].

The rest of the article is organized as follows. Details of the method are outlined in sections 2 and 3; specific details on q POTS is provided in section 2.3. The numerical experiments are presented in section 4. We provide concluding remarks and an outlook for future work in section 5.

2 Methodology

2.1 Single objective Bayesian optimization

We place an independent GP prior on the oracle $f(\mathbf{x}) \sim \mathcal{GP}(0, k(\mathbf{x}, \cdot))$, where $k(\cdot, \cdot) : \mathcal{X} \times \mathcal{X} \rightarrow \mathbb{R}_+$ is a covariance function (a.k.a., *kernel*). We denote the observations from the oracle as $y_i = f(\mathbf{x}_i) + \epsilon_i$, $i = 1, \dots, n$, where we assume that ϵ_i is Gaussian with zero-mean and unknown variance τ^2 , which could be input dependent (i.e., heteroscedastic). We begin by fitting a GP (parametrized by hyperparameters Ω) for the observations $\mathcal{D}_n = \{\mathbf{x}_i, y_i, \tau^2\}$, $i = 1, \dots, n$, which gives the conditional aposteriori distribution [43]

$$\begin{aligned} Y(\mathbf{x})|\mathcal{D}_n, \Omega &\sim \mathcal{GP}(\mu_n(\mathbf{x}), \sigma_n^2(\mathbf{x})), \\ \mu_n(\mathbf{x}) &= \mathbf{k}_n^\top [\mathbf{K}_n + \tau^2 \mathbf{I}]^{-1} \mathbf{y}_n \\ \sigma_n^2(\mathbf{x}) &= k(\mathbf{x}, \mathbf{x}) - \mathbf{k}_n^\top [\mathbf{K}_n + \tau^2 \mathbf{I}]^{-1} \mathbf{k}_n, \end{aligned} \quad (1)$$

where \mathbf{k}_n is a vector of covariances between \mathbf{x} and all observed points in \mathcal{D}_n , \mathbf{K}_n is a sample covariance matrix of observed points in \mathcal{D}_n , \mathbf{I} is the identity matrix, and \mathbf{y}_n is the vector of all observations in \mathcal{D}_n . We also denote by $X_n = [\mathbf{x}_1, \dots, \mathbf{x}_n]^\top \in \mathbb{R}^{n \times d}$ to refer to all the observation sites. BO seeks to make sequential decisions based on a probabilistic utility function constructed out of the posterior GP $u(\mathbf{x}) = u(Y(\mathbf{x})|\mathcal{D}_n)$. Sequential decisions are the result of an "inner" optimization subproblem that optimizes an acquisition function, typically, of the form $\alpha(\mathbf{x}) = \mathbb{E}_{Y|\mathcal{D}_n}[u(Y(\mathbf{x}))]$. For example, the EI [30] and PI [37] can be expressed as $\alpha_{\text{PI}}(\mathbf{x}) = \mathbb{E}_{Y|\mathcal{D}_n}[(Y(\mathbf{x}) - \xi)]$ and $\alpha_{\text{EI}}(\mathbf{x}) = \mathbb{E}_{Y|\mathcal{D}_n}[\max(0, (Y(\mathbf{x}) - \xi))]$, respectively, where ξ is a target value. Although α_{EI} and α_{PI} have analytically closed and continuously differential forms, their batch-acquisition variants are not necessarily [21]. Further, the information theoretic approaches [24, 25, 56], also typically require approximations and/or Monte Carlo sampling, making them computationally expensive and hard to optimize.

An approach that circumvents the acquisition function construction is Thompson sampling (TS) [54]. TS proposes making a decision according to the probability that it is optimal in some sense [45]. In (single objective) optimization, points are chosen according to the distribution $p_{\mathbf{x}^*}(\mathbf{x})$, where \mathbf{x}^* is the optimizer of the objective function. In the context of BO, this can be expressed as

$$\begin{aligned} p_{\mathbf{x}^*}(\mathbf{x}) &= \int p_{\mathbf{x}^*}(\mathbf{x}|Y)p(Y|\mathcal{D}_n)dY \\ &= \int \delta(\mathbf{x} - \arg \max_{\mathbf{x} \in \mathcal{X}} Y(\mathbf{x}))p(Y|\mathcal{D}_n)dY, \end{aligned} \quad (2)$$

where δ is the Dirac delta function. Sampling from $p_{\mathbf{x}^*}(\mathbf{x})$ is equivalent to finding the maximizer of a sample path $Y(\cdot, \omega)$, where ω is the random parameter. Our proposed approach builds on TS which we present next.

2.2 Multiobjective Bayesian optimization

We first fit K independent posterior GP models: $\mathcal{M}_1, \dots, \mathcal{M}_K$ for the K objectives, with observations $\mathcal{D}_n^{1:K} \triangleq \{\mathcal{D}_n^1, \dots, \mathcal{D}_n^K\}$. In the multiobjective setting, acquisition functions are typically defined in terms of a hypervolume (HV) indicator. HV of a Pareto frontier \mathcal{P} is the K -dimensional Lebesgue measure λ of the region dominated by its Pareto set \mathcal{P} and bounded from below by a reference point $\mathbf{r} \in \mathbb{R}^K$. That is, $HV(\mathcal{P}|\mathbf{r}) = \lambda_K(\bigcup_{\nu \in \mathcal{P}} [\mathbf{r}, \nu])$, where $[\mathbf{r}, \nu]$ denotes the hyper-rectangle bounded by vertices \mathbf{r} and ν ; see [13]. EHVI [8, 17] computes the expectation (with respect to the posterior GP) of the improvement in HV due to a candidate point. Our approach, however, does not

involve the computation of HV but is an extension of (2) to the multiobjective setting.

2.3 qPOTS: Pareto optimal Thompson sampling for multiobjective BO

Inspired from TS, qPOTS chooses points according to the probability that they are Pareto optimal. That is, we choose \mathbf{x} according to the probability

$$p_{\mathcal{X}^*}(\mathbf{x}) = \int \delta \left(\mathbf{x} - \arg \max_{\mathbf{x} \in \mathcal{X}} \{Y_1(\mathbf{x}), \dots, Y_K(\mathbf{x})\} \right) p(Y_1 | \mathcal{D}_n^1) \dots p(Y_K | \mathcal{D}_n^K) dY_1 \dots dY_K,$$

where the integral is over the support of the joint distribution of all posterior GPs. In practice, this is equivalent to drawing sample paths from the K posterior GPs $Y_i(\cdot, \omega)$, $i = 1, \dots, K$, and choosing the next point(s) from its Pareto set $\mathbf{x}_{n+1} \in \arg \max_{\mathbf{x} \in \mathcal{X}} \{Y_1(\mathbf{x}, \omega), \dots, Y_K(\mathbf{x}, \omega)\}$. We use the ‘‘reparametrization trick’’ to sample from the posterior (again we exclude notations for individual objectives): $Y(\cdot, \omega) = \mu_n(\cdot) + \Sigma_n^{1/2}(\cdot) \times Z(\omega)$, where Z is a standard multivariate normal random variable. Then, we solve the following cheap multiobjective optimization problem

$$X^* = \arg \max_{\mathbf{x} \in \mathcal{X}} \{Y_1(\mathbf{x}, \omega), \dots, Y_K(\mathbf{x}, \omega)\}, \quad (3)$$

that can be solved using evolutionary such as NSGA-II [14]. The next batch of q points is then chosen as $\mathbf{x}_{n+1:q} \in X^*$. That is, we select points from the predicted Pareto set of the sample paths of each posterior GP. The acquisition assumes $q \leq N^* = |X^*|$; we provide some measures a user can take to ensure the pathology $q > N^*$ is overcome in practice, in Section 3.4. The solution to (3) via NSGA-II involves the specification of a population size \tilde{N} , which is the number of evaluations in \mathcal{X} made for each posterior GP per generation, and a generation size N_{gen} , which is the number of mutated and crossed-over generations of samples used in NSGA-II; see [14]. \tilde{N} affects the computational efficiency of qPOTS, and we discuss this, and associated measures, in Section 3. Additionally, using a finite number (\tilde{N}) of points in \mathcal{X} introduces an approximation to (3). That is,

$$\mathbf{x}_{n+1:q} \in \tilde{X}^* = \arg \max_{\mathbf{x} \in \tilde{\mathcal{X}}} \{Y_1(\mathbf{x}, \omega), \dots, Y_K(\mathbf{x}, \omega)\} \approx X^*. \quad (4)$$

The Pareto set in $\tilde{\mathcal{X}}$ then serves as an approximation to the true Pareto set. We use the approach in [33] to identify local lower bounds of the posterior GP sampled on $\tilde{\mathcal{X}}$. We then use the box-decomposition technique in [60] to partition the dominated space by the local lower bounds using axis-aligned hyperrectangles that

are used to compute the hypervolume, for downstream postprocessing.

Additionally, we take a measure to avoid new acquisitions to be too close to existing observed sites as it leads to ill-conditioning of the posterior GP covariance matrix. In this regard, we ensure that the acquisition \mathbf{x}_{n+1} has the largest *maximin distance* [28, 51] to the previously observed points. With a slight abuse of notation, let $\delta(\cdot, \cdot) : \mathbb{R}^d \times \mathbb{R}^d \rightarrow \mathbb{R}_+$ denote the Euclidean distance between two points in \mathcal{X} . Then, we pick the q new acquisitions according to

$$\begin{aligned} \mathbf{x}_{n+1} &= \max_{\tilde{\mathbf{x}}^* \in \tilde{X}^*} \min_{\mathbf{x}_i \in X_n} \delta(\tilde{\mathbf{x}}^*, \mathbf{x}_i) \\ \mathbf{x}_{n+2} &= \max_{\tilde{\mathbf{x}}^* \in \tilde{X}^*} \min_{\mathbf{x}_i \in X_n \cup \mathbf{x}_{n+1}} \delta(\tilde{\mathbf{x}}^*, \mathbf{x}_i) \\ &\vdots \\ \mathbf{x}_{n+q} &= \max_{\tilde{\mathbf{x}}^* \in \tilde{X}^*} \min_{\mathbf{x}_i \in X_n \cup \{\mathbf{x}_{n+1}, \dots, \mathbf{x}_{n+q-1}\}} \delta(\tilde{\mathbf{x}}^*, \mathbf{x}_i). \end{aligned} \quad (5)$$

In practice, (5) involves the computation of an $\tilde{N}^* \times n$ pairwise distance matrix ($\tilde{N}^* = |\tilde{X}^*|$) and rank-ordering them to according to their column-wise minima. An ascending sort of the resulting vector allows for selecting the q batch acquisition as the last q elements of the sorted vector. Our overall algorithm is endowed with a rather straightforward implementation and is summarized in Algorithm 1.

3 Computational scaling and practical considerations

The size of the candidate set \tilde{N} is a parameter in our approach. Naturally, large d requires large \tilde{N} , and thus this introduces a scalability issue that must be addressed. Specifically, sampling the posterior GP requires a matrix square root $\Sigma_{\tilde{N}}^{1/2} = (\mathbf{K}_{\tilde{N}} + \tau^2 \mathbf{I})^{1/2}$, which has a complexity of $\mathcal{O}(\tilde{N}^3)$. We address this via the following techniques.

3.1 Computational complexity

The cost of computing the posterior covariance matrix, per objective, is $\mathcal{O}(\tilde{N}^2 n)$ when $\tilde{N} \gg n$ and $\mathcal{O}(\tilde{N} n^2)$ when $n \gg \tilde{N}$. In practice, for engineering problems, n is often modest (< 1000) but \tilde{N} can quickly explode with increasing d . In our approach, where we use a candidate set $\tilde{\mathcal{X}}$, typically $\tilde{N} \gg n$ and thus we need strategies to address the complexity of operating on the posterior GP evaluated on \tilde{X} . Therefore, we address the scaling issue by reducing \tilde{N} rather than n . In this regard, we propose a Nyström-like approximation to the posterior covariance matrix based on an *active set* $\tilde{\mathcal{X}}_r$ of the candidates in $\tilde{\mathcal{X}}$ selected using an accept-reject algorithm, where $|\tilde{\mathcal{X}}_r| = m < \tilde{N}$. Then, a Nyström

Algorithm 1: q POTS: Pareto optimal Thompson sampling

- 1 **Given:** With data sets $\mathcal{D}_n^{1:K}$, fit K GP models \mathcal{M}_1 through \mathcal{M}_K and GP hyperparameters $\Omega_1, \dots, \Omega_K$.
 - 2 Parameters $\tilde{N}, N_{\text{gen}}, B$ (total budget)
 - Result:** Pareto optimal designs $\tilde{\mathcal{X}}^*$
 - 3 **for** $i = n + 1, \dots, B$, **do**
 - 4 Solve a cheap multiobjective optimization problem via NSGA-II with a population size \tilde{N} for N_{gen} generations
 $\tilde{X}^* = \arg \max_{\mathbf{x} \in \tilde{\mathcal{X}}} \{Y_1(\tilde{\mathcal{X}}), \dots, Y_K(\tilde{\mathcal{X}})\}$.
 - 5 **(Optional)** Nyström with active candidate set: sample the posterior GPs directly on the active set $\tilde{\mathcal{X}}_r$ (Algorithm 2) with Nyström approximation Section 3.3.
 - 6 Choose $q \leq \tilde{N}$ candidate points from $\tilde{\mathcal{X}}^*$ in decreasing order of maximin distance to X_n , according to (5).
 - 7 Observe oracles $f_i(\mathbf{x}_{n+1}), \dots, f_i(\mathbf{x}_{n+q})$, and append data set $\mathcal{D}_i \cup \{(\mathbf{x}_{n+1}, f_i(\mathbf{x}_{n+1})), \dots, (\mathbf{x}_{n+q}, f_i(\mathbf{x}_{n+q}))\}$, $\forall i = 1, \dots, K$.
 - 8 Update GP hyperparameters $\Omega_1, \dots, \Omega_K$
-

approximation $\tilde{\Sigma}(\tilde{\mathcal{X}})$ of the full covariance matrix is constructed using the m points in $\tilde{\mathcal{X}}_r$. We now provide details on both of these approaches.

3.2 Active set selection via accept-reject sampling

The intuition for this is that the Pareto set is likely clusters of small, contiguous sets of points. Therefore, candidates in the neighborhood of these sets are most important in generating posterior samples and, vice versa, points far away from the Pareto set are less important. In this regard, we propose an accept-reject sampling approach [44, 23], which sub-samples a dense candidate set such that candidates closer to the Pareto set are retained, whereas points far away are coarsely sampled; this is in the same spirit as the *subset of data points* approach shown in [34, 48]. The key aspect worth mentioning here is that candidates far away from the current predicted Pareto set must still be sampled, albeit coarsely, to retain the exploratory nature of the proposed method. This is described as follows. Let the candidate set $\tilde{\mathcal{X}}$ be generated from a distribution $p_{\tilde{\mathcal{X}}}$. Furthermore, let $p_{\mathcal{X}^*}$ denote the distribution of the Pareto set; our goal is to *filter* the candidate set according to the probability of being Pareto optimal. That is, we *reject* samples which have low probability of being Pareto optimal. This is done in the following

Algorithm 2: Accept-reject sampling for active set selection

- 1 **Given:** Candidate set $\tilde{\mathcal{X}}$, observed points $\mathcal{D}_n^{1:K}$, current nondominated set $X_{\text{nd}} \subset X_n$, bandwidth parameter h
 - Result:** Active set $\tilde{\mathcal{X}}_r$, $|\tilde{\mathcal{X}}_r| = m < \tilde{N}$
 1. Construct a KDE of $p_{\mathcal{X}^*}$ using X_{nd} (Equation (6))
 2. Draw \tilde{N} samples U_i , $i = 1, \dots, \tilde{N}$ uniformly at random
 3. Reject samples in $\tilde{\mathcal{X}}$ according to the probability U_i . That is, if $U_i < p_{\mathcal{X}^*}(\tilde{\mathbf{x}}_i)$, accept $\tilde{\mathbf{x}}_i$, $\forall i = 1, \dots, \tilde{N}$, else reject.
 4. Return accepted set $\tilde{\mathcal{X}}_r$.
-

steps in Algorithm 2. This way, we end up with a candidate set $\tilde{\mathcal{X}}_r \subset \tilde{\mathcal{X}}$ and, more importantly, $|\tilde{\mathcal{X}}_r| \ll |\tilde{\mathcal{X}}|$. The key question now is: how to get the distribution $p_{\mathcal{X}^*}$? For this, we provide an inverse-distance weighted kernel density estimate (KDE) defined as follows

$$\hat{p}_{\tilde{\mathcal{X}}^*}(\mathbf{x}) = \frac{1}{N_{\text{nd}}} \sum_{i=1}^{N_{\text{nd}}} K_h(\|\mathbf{x} - \mathbf{x}_i\|), \quad (6)$$

where K_h is an inverse-distance weighted kernel, $\|\cdot\|$ is the Euclidean norm, and N_{nd} denotes the cardinality of the nondominated set within all the observed points X_n . We pick K_h to be the squared-exponential kernel $K_h(\|\mathbf{x} - \mathbf{x}_i\|) = \exp\left(-\frac{\|\mathbf{x} - \mathbf{x}_i\|^2}{2h^2}\right)$, where h is a bandwidth parameter, which satisfies the inverse-distance weighting that we expect. Smaller h filters aggressively resulting in smaller m . For a normalized domain $\mathcal{X} = [0, 1]^d$, we have observed $0.05 \leq h \leq 0.1$ to be sufficient; $h = 0.1$ worked uniformly well for all our experiments. Therefore, the idea is to weight the candidates closer to the observed nondominated set higher compared to those that are farther away. Then, in step 2 of Algorithm 2, we use the probability score from $\hat{p}_{\tilde{\mathcal{X}}^*}(\mathbf{x})$ instead of $p_{\tilde{\mathcal{X}}^*}(\mathbf{x})$. A demonstration of the proposed rejection sampling approach is shown in Figure 1. With the active set $\tilde{\mathcal{X}}_r$ extracted from Algorithm 2, we are ready to construct the Nyström approximation described next.

3.3 Nyström approximation on active candidate set

Recall that $m < \tilde{N}$ denotes the cardinality of $\tilde{\mathcal{X}}_r$ that we subsample from $\tilde{\mathcal{X}}$. We choose the elements of $\tilde{\mathcal{X}}_r$ in one shot using Algorithm 2, but other, adaptive, forward selection (a.k.a, greedy sampling) strategies

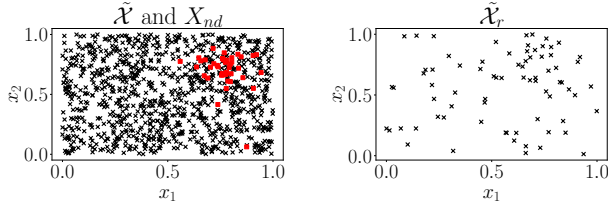


Figure 1: Illustration of Algorithm 2. Left: candidates (black) and current nondominated set (red). Right: subsampled active set $\tilde{\mathcal{X}}_r$. $|\tilde{\mathcal{X}}_r| \approx 6\%$ of $|\tilde{\mathcal{X}}|$.

also exist [49, 19, 16]. The main idea we propose is that we will compute the eigen decomposition of the $m \times m$ posterior covariance matrix and use Nyström approximation to approximate the full $\tilde{N} \times \tilde{N}$ matrix. This view was presented by [57] and is explained as follows; for alternate views, see [49, 47]. We first partition $\Sigma(\tilde{\mathcal{X}})$ as follows

$$\Sigma(\tilde{\mathcal{X}}) = \begin{bmatrix} \Sigma_{mm} & \Sigma_{m(\tilde{N}-m)} \\ \Sigma_{(\tilde{N}-m)m} & \Sigma_{(\tilde{N}-m)(\tilde{N}-m)} \end{bmatrix}$$

and compute the eigen decomposition of Σ_{mm} —denote the eigenvalues an eigenvectors as $\{\lambda_i^{(m)}, i = 1, \dots, m\}$ and $\{\mathbf{u}_i^{(m)}, i = 1, \dots, m\}$, respectively. Then, this is extended to incorporate all \tilde{N} points as

$$\begin{aligned} \tilde{\lambda}_i^{(\tilde{N})} &= \frac{\tilde{N}}{m} \lambda_i^{(m)}, i = 1, \dots, m \\ \tilde{\mathbf{u}}_i^{(\tilde{N})} &= \sqrt{\frac{m}{\tilde{N}}} \frac{1}{\sqrt{\lambda_i^{(m)}}} \Sigma_{m(\tilde{N}-m)} \mathbf{u}_i^{(m)}, i = 1, \dots, m. \end{aligned}$$

Then, the Nyström approximation to Σ is given by

$$\tilde{\Sigma}(\tilde{\mathcal{X}}) = \Sigma_{\tilde{N}m} \Sigma_{mm}^{-1} \Sigma_{m\tilde{N}},$$

where $\Sigma_{m\tilde{N}}$ is the upper $m \times \tilde{N}$ block of $\Sigma(\tilde{\mathcal{X}})$. The Nyström approximation costs $\mathcal{O}(m^2\tilde{N})$, which is significantly reduced since it is linear in \tilde{N} .

3.4 Avoiding pathologies with batch sampling

Finally, we address an important practical consideration. Since we operate with a candidate set $\tilde{\mathcal{X}}$, there is no guarantee that the resulting nondominated set $\tilde{\mathcal{X}}^*$ has higher cardinality than q . Therefore, when $q > |\tilde{\mathcal{X}}^*|$, we use the following procedure, that guarantees sampling a batch of q points in every step. Firstly, we choose all of the $q^{(1)} = |\tilde{\mathcal{X}}^*|$ points and append them to the observed set X_n . Then, we solve (4) again, with a new set of posterior GP covariance matrices, to select a new batch of $q^{(2)}$ points that have the highest maximin distance with respect to the augmented set $X_n \cup \tilde{\mathcal{X}}_{n+1}^*$. We repeat this process until $\sum_i q^{(i)} = q$.

4 Experiments

We demonstrate our methodology on several synthetic and real-world experiments ranging from $d = 2$ through $d = 10$ as well as $K = 2$ through $K = 4$. We compare qPOTS against qNEHVI, qParEGO, PESMO, JESMO, MESMO, and random Sobol sampling. For the synthetic experiments, we use the 2D Branin-Currian ($d = 2, K = 2$); DTLZ1 test function [15] ($d=3,5,10; K=2$). For the real-world experiment, we use the Vehicle Safety problem [53] and the Penicillin production problem [35], and the Car side-impact problem [27]. The Penicillin production problem ($d = 7, K = 3$) seeks to maximize Penicillin yield while minimizing the time for production as well as the carbon dioxide byproduct emission. The $d = 7$ input variables include the culture medium volume, biomass concentration, temperature K , glucose substrate concentration, substrate feed rate, substrate feed concentration and the $H+$ concentration [35]. The Vehicle Safety problem ($d = 5, K = 3$) [53] concerns the design of automobiles for enhanced safety. Specifically, we consider the minimization of vehicle mass, the vehicle acceleration during a full-frontal crash, and the toe-board intrusion—a measure of the mechanical damage to the vehicle during an off-frontal crash, with respect to 5 design variables which represent the reinforced parts of the frontal frame. Mathematical formulations of the 3 objectives are found in the original study [36]. The Car side-impact problem is aimed at minimizing the weight of the car while minimizing the pubic force experienced by a passenger and the average velocity of the V-pillar responsible for withstanding the impact load. Additionally, as the fourth objective, the maximum constraint violation of 10 constraints which include limiting values of abdomen load, pubic force, velocity of V-pillar, and rib deflection is also added [27].

We provide each experiment a set of seed samples and observations to start the algorithm, chosen uniformly at random from \mathcal{X} . For the 2D experiments ($K = 2$), we start with 5 samples and run for an additional 50 iterations, for the 3D and 5D experiments, we start with 30 and 50 points, respectively, and run for 100 iterations; for the 10D experiment we start with 100 points and run for 200 iterations. All experiments are repeated 10 times, each repetition receiving a unique set of seed samples which are common for each acquisition function. We add a Gaussian noise with variance $\tau^2 = 10^{-3}$ to all our observations. The experiments are run with a high-performance compute node with 256gb memory and 10 CPU cores to parallelize the repetitions. Our metric for comparison is the hypervolume computed via box decomposition [60]; we generate a dense candidate set of $1000 \times d$ points via LHS in \mathcal{X} to compute the *true* hypervolume with the actual oracles $f_i, i = 1, \dots, K$; we then use the log of the normalized

hypervolume difference $1 - \frac{HV_{\text{predicted}}}{HV_{\text{true}}}$ to compare our strategy with others. In addition to the hypervolume, we also monitor the cumulative CPU time to quantify the computational speed-up we achieve from our strategy. We compare our strategy against two classical methods: qNEHVI and qNParEGO, three state-of-the-art entropy-based methods: PESMO, MESMO, and JESMO, as well as a random strategy via Sobol sampling; comparison beyond the chosen methods has been limited by the non-availability of the source codes at the moment of writing this manuscript. Throughout the manuscript, we default to the anisotropic Matern class kernel with $\nu = 5/2$. Our implementation primarily builds on GPyTorch [20] and BoTorch [1]; we leverage PyKeOPs [6] to efficiently compute and operate on the covariance matrices as well as pairwise distances and we use MPI4Py [9] to parallelize our repetitions. We use PyMOO [3] to leverage its NSGA-II solver. The full source code to reproduce our results will be made available upon publication of this manuscript.

Figure 3 shows the performance comparison on the synthetic experiments; top row shows the log difference in hypervolume (lower the better) and bottom row the cumulative CPU time (also lower the better) taken by each algorithm. Notice that $qPOTS$ outperforms other strategies in all but the ZLDT1-10D, in which case, it is marginally outperformed by PESMO. More for $d < 10$, $qPOTS$ is an order of magnitude faster than others and is in fact on the same order of magnitude as Sobol. At $d = 10$, $qPOTS$ becomes computationally expensive, yet no worse than JESMO. In higher dimensions, a simple strategy to compensate for the computational cost of $qPOTS$ is to sample in batches; this is demonstrated in Figure 2—notice that the cost of $q = 4$ and $q = 1$ are almost indistinguishable. Finally, notice that $qPOTS$ -Nyström significantly speeds up $qPOTS$ for a small trade in accuracy.

The demonstration on the real-world experiments is shown in Figure 4. Notice that $qPOTS$ comfortably outperforms all competitors in both the Vehicle Safety and Car Side-Impact problems; while still outperforming others in the Penicillin problem. While the only drawback is the computational cost of $qPOTS$, which quickly increases with d , it is still no worse than the information theoretic policies: PESMO, MESMO, and JESMO. Nevertheless, as described and demonstrated previously, with active set selection and the Nyström approximation, the computations in $qPOTS$ can be drastically sped-up for a small trade in accuracy. We reiterate that $qPOTS$ works for arbitrary GP kernels and nonstationary approaches (deep GPs), unlike RFF.

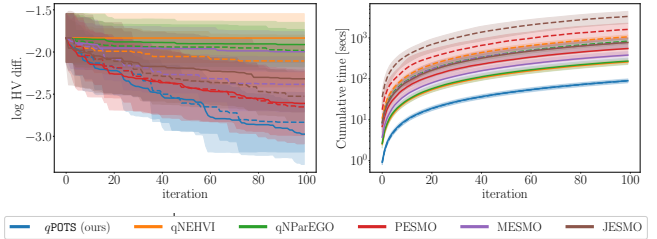


Figure 2: **Batch Vs. sequential acquisition** (on the DTLZ1-3D function). Left: log HV difference, right: cumulative CPU time. Solid lines represent $q = 1$ and dashed lines $q = 4$. Notice that, whereas sequential and batch sampling costs almost the same for $qPOTS$, they could be an order of magnitude higher for others.

5 Discussion

We have presented $qPOTS$, an efficient MOBO method to solve multiobjective optimization with expensive oracles. Our work is motivated by a limitation with existing MOBO methods, where a nonconvex, possibly non-smooth and stochastic inner optimization is necessary and the success of the overall method relies on the accuracy of this inner optimization. Unlike existing methods, $qPOTS$ relies on sampling from the posterior GPs, and solving a cheap multiobjective optimization on the posterior sample paths with classical evolutionary algorithms such as NSGA-II. This way, we bridge the gap between classical EA’s and MOBO and thus, in a sense, getting the best of both worlds. $qPOTS$ returns a random Pareto frontier, from which future observation sites can be chosen. This randomness in the obtained Pareto frontier is governed by the inherent uncertainty in the posterior GPs and hence naturally trades exploration and exploitation. More importantly, batch acquisition ($q > 1$) comes at the same cost as sequential acquisition ($q = 1$). The main limitation of our approach is the scaling at higher dimensions due to the covariance matrix square-root. However, we have demonstrated that the approximation via $qPOTS$ -Nyström significantly reduces the computational overhead for a potentially small trade in accuracy. Crucially, our approach freely applies to any covariance kernel (unlike RFF for stationary kernels) and non-Gaussian models such as deep GPs.

Looking into the future, one avenue of interest is exploring the full extent of GPU acceleration, particularly with multi-GPU computations. Secondly, marrying $qPOTS$ with deep GPs would open doors for more applications where nonstationarity in the oracles is expected to be strong. Finally, we are interested in establishing the theoretical guarantees with $qPOTS$.

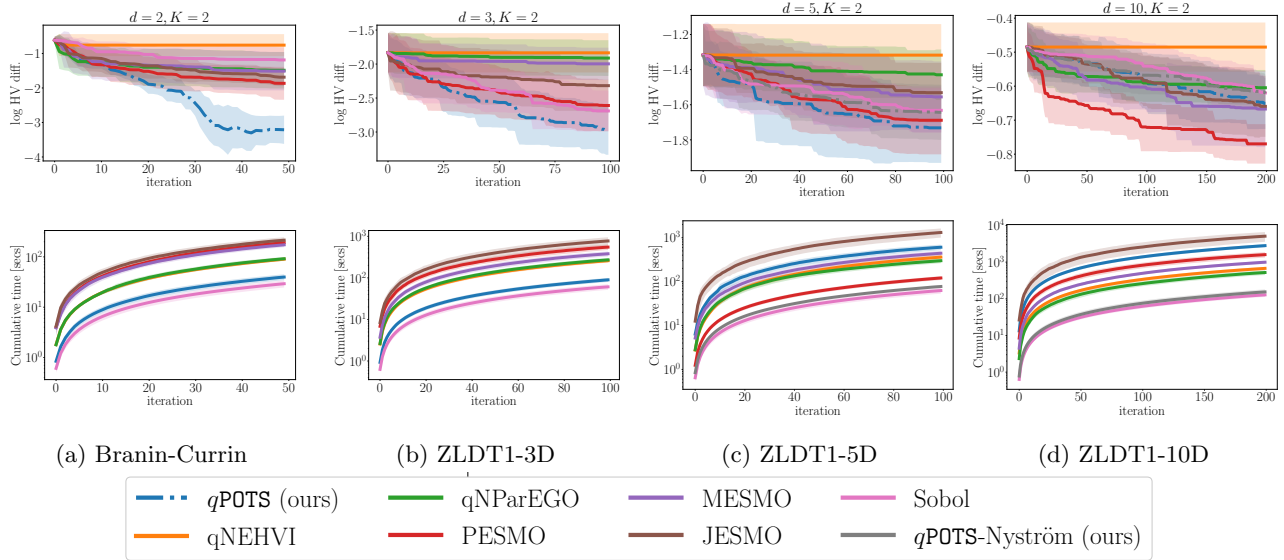


Figure 3: **Synthetic experiments.** Top row: log hypervolume difference; bottom row: cumulative CPU time until current iteration. In lower dimensions, *q*POTS is almost as fast as random sampling (Sobol). When $d = 10$, *q*POTS becomes computationally expensive but no worse than JESMO. Note that *q*POTS-Nyström significantly speeds up *q*POTS for a small trade in accuracy. All experiments use sequential ($q = 1$) acquisition.

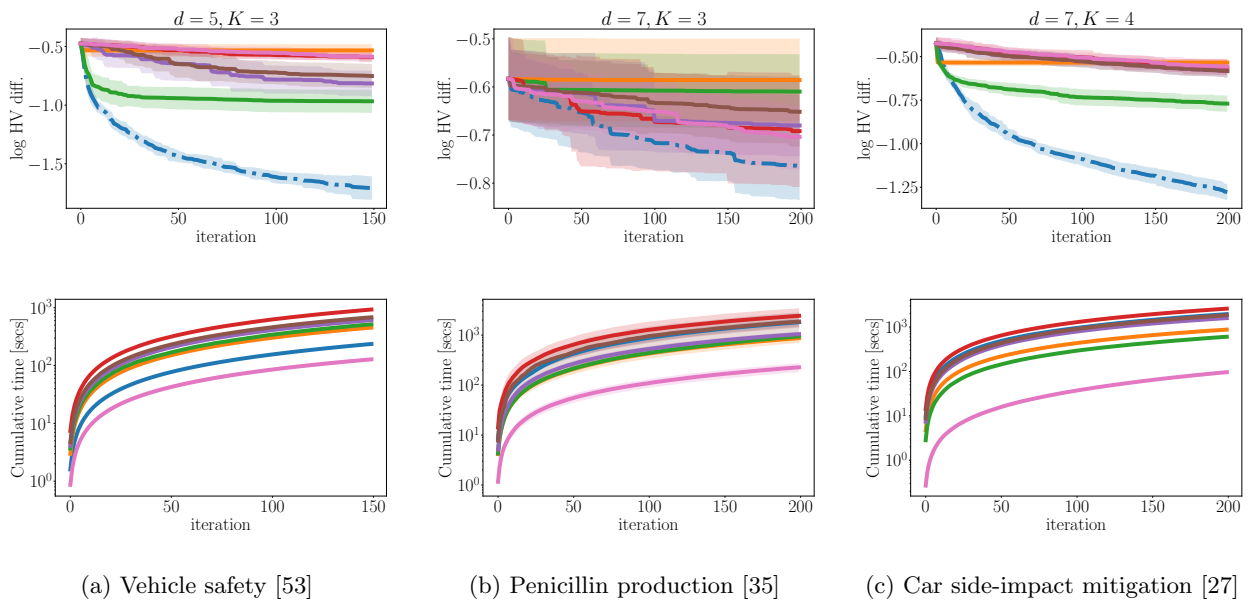


Figure 4: **Real-world experiments.** *q*POTS outperforms all the competing methods. All experiments use sequential ($q = 1$) acquisition. Legend is per Figure 3.

References

- [1] Maximilian Balandat, Brian Karrer, Daniel R Jiang, Samuel Daulton, Benjamin Letham, Andrew Gordon Wilson, and Eytan Bakshy. BoTorch: Programmable Bayesian optimization in PyTorch. *arXiv:1910.06403*, 2019.
- [2] Syrine Belakaria, Aryan Deshwal, and Janardhan Rao Doppa. Max-value Entropy Search for Multi-Objective Bayesian Optimization. In *Advances in Neural Information Processing Systems*, volume 32. Curran Associates, Inc., 2019.
- [3] Julian Blank and Kalyanmoy Deb. Pymoo: Multi-objective optimization in python. *Ieee access*, 8:89497–89509, 2020.
- [4] Annie S Booth, S Ashwin Renganathan, and Robert B Gramacy. Contour location for reliability in airfoil simulation experiments using deep gaussian processes. *arXiv preprint arXiv:2308.04420*, 2023.
- [5] Eric Bradford, Artur M Schweidtmann, and Alexei Lapkin. Efficient multiobjective optimization employing gaussian processes, spectral sampling and a genetic algorithm. *Journal of global optimization*, 71(2):407–438, 2018.
- [6] Benjamin Charlier, Jean Feydy, Joan Alexis Glaunes, François-David Collin, and Ghislain Durif. Kernel operations on the gpu, with autodiff, without memory overflows. *The Journal of Machine Learning Research*, 22(1):3457–3462, 2021.
- [7] Clément Chevalier, Julien Bect, David Ginsbourger, Emmanuel Vazquez, Victor Picheny, and Yann Richet. Fast parallel kriging-based stepwise uncertainty reduction with application to the identification of an excursion set. *Technometrics*, 56(4):455–465, 2014.
- [8] Ivo Couckuyt, Dirk Deschrijver, and Tom Dhaene. Fast calculation of multiobjective probability of improvement and expected improvement criteria for Pareto optimization. *Journal of Global Optimization*, 60(3):575–594, November 2014.
- [9] Lisandro Dalcin and Yao-Lung L Fang. mpi4py: Status update after 12 years of development. *Computing in Science & Engineering*, 23(4):47–54, 2021.
- [10] Andreas Damianou and Neil D Lawrence. Deep gaussian processes. In *Artificial intelligence and statistics*, pages 207–215. PMLR, 2013.
- [11] Samuel Daulton, Maximilian Balandat, and Eytan Bakshy. Differentiable expected hypervolume improvement for parallel multi-objective bayesian optimization. *Advances in Neural Information Processing Systems*, 33:9851–9864, 2020.
- [12] Samuel Daulton, Maximilian Balandat, and Eytan Bakshy. Differentiable Expected Hypervolume Improvement for Parallel Multi-Objective Bayesian Optimization. In *Advances in Neural Information Processing Systems*, volume 33, pages 9851–9864. Curran Associates, Inc., 2020.
- [13] Samuel Daulton, Maximilian Balandat, and Eytan Bakshy. Parallel Bayesian Optimization of Multiple Noisy Objectives with Expected Hypervolume Improvement. In *Advances in Neural Information Processing Systems*, volume 34, pages 2187–2200. Curran Associates, Inc., 2021.
- [14] Kalyanmoy Deb, Amrit Pratap, Sameer Agarwal, and TAMI Meyarivan. A fast and elitist multiobjective genetic algorithm: Nsga-ii. *IEEE transactions on evolutionary computation*, 6(2):182–197, 2002.
- [15] Kalyanmoy Deb, Lothar Thiele, Marco Laumanns, and Eckart Zitzler. Scalable test problems for evolutionary multiobjective optimization. In *Evolutionary multiobjective optimization: theoretical advances and applications*, pages 105–145. Springer, 2005.
- [16] Petros Drineas and Michael W Mahoney. Approximating a gram matrix for improved kernel-based learning. In *International Conference on Computational Learning Theory*, pages 323–337. Springer, 2005.
- [17] Michael Emmerich. The computation of the expected improvement in dominated hypervolume of Pareto front approximations. January 2008.
- [18] Peter I Frazier, Warren B Powell, and Savas Dayanik. A knowledge-gradient policy for sequential information collection. *SIAM Journal on Control and Optimization*, 47(5):2410–2439, 2008.
- [19] Alan Frieze, Ravi Kannan, and Santosh Vempala. Fast monte-carlo algorithms for finding low-rank approximations. *Journal of the ACM (JACM)*, 51(6):1025–1041, 2004.
- [20] Jacob Gardner, Geoff Pleiss, Kilian Q Weinberger, David Bindel, and Andrew G Wilson. GPyTorch: Blackbox matrix-matrix Gaussian process inference with GPU acceleration. In *Advances in Neural Information Processing Systems*, pages 7576–7586, 2018.

- [21] David Ginsbourger and Rodolphe Le Riche. Towards Gaussian process-based optimization with finite time horizon. In *Contributions to Statistics*, pages 89–96. Springer, 2010.
- [22] Robert B Gramacy, Annie Sauer, and Nathan Wycoff. Triangulation candidates for bayesian optimization. *Advances in Neural Information Processing Systems*, 35:35933–35945, 2022.
- [23] John Hammersley. *Monte carlo methods*. Springer Science & Business Media, 2013.
- [24] Daniel Hernández-Lobato, José Miguel Hernández-Lobato, Amar Shah, and Ryan P Adams. Predictive Entropy Search for Multi-objective Bayesian Optimization.
- [25] José Miguel Hernández-Lobato, Matthew W. Hoffman, and Zoubin Ghahramani. Predictive entropy search for efficient global optimization of black-box functions. In *Advances in Neural Information Processing Systems*, pages 918–926, 2014.
- [26] Carl Hvarfner, Frank Hutter, and Luigi Nardi. Joint entropy search for maximally-informed bayesian optimization. *Advances in Neural Information Processing Systems*, 35:11494–11506, 2022.
- [27] Himanshu Jain and Kalyanmoy Deb. An evolutionary many-objective optimization algorithm using reference-point based nondominated sorting approach, part ii: Handling constraints and extending to an adaptive approach. *IEEE Transactions on evolutionary computation*, 18(4):602–622, 2013.
- [28] Mark E. Johnson, Leslie M. Moore, and Donald Ylvisaker. Minimax and maximin distance designs. *Journal of Statistical Planning and Inference*, 26(2):131–148, 1990.
- [29] Donald R. Jones. A taxonomy of global optimization methods based on response surfaces. *Journal of Global Optimization*, 21(4):345–383, 2001.
- [30] Donald R. Jones, Matthias Schonlau, and William J. Welch. Efficient global optimization of expensive black-box functions. *Journal of Global Optimization*, 13(4):455–492, 1998.
- [31] Joshua Knowles. Parego: A hybrid algorithm with on-line landscape approximation for expensive multiobjective optimization problems. *IEEE Transactions on Evolutionary Computation*, 10(1):50–66, 2006.
- [32] Mina Konakovic Lukovic, Yunsheng Tian, and Wojciech Matusik. Diversity-Guided Multi-Objective Bayesian Optimization With Batch Evaluations. In *Advances in Neural Information Processing Systems*, volume 33, pages 17708–17720. Curran Associates, Inc., 2020.
- [33] Renaud Lacour, Kathrin Klamroth, and Carlos M Fonseca. A box decomposition algorithm to compute the hypervolume indicator. *Computers & Operations Research*, 79:347–360, 2017.
- [34] Neil Lawrence, Matthias Seeger, and Ralf Herbrich. Fast Sparse Gaussian Process Methods: The Informative Vector Machine. In *Advances in Neural Information Processing Systems*, volume 15. MIT Press, 2002.
- [35] Qiaohao Liang and Lipeng Lai. Scalable bayesian optimization accelerates process optimization of penicillin production. In *NeurIPS 2021 AI for Science Workshop*, 2021.
- [36] Xingtao Liao, Qing Li, Xujing Yang, Weigang Zhang, and Wei Li. Multiobjective optimization for crash safety design of vehicles using stepwise regression model. *Structural and multidisciplinary optimization*, 35:561–569, 2008.
- [37] Jonas Mockus, Vytautas Tiešis, and Antanas Žilinskas. The application of Bayesian methods for seeking the extremum. *Towards Global Optimization*, 2:117–129, 1978.
- [38] Biswajit Paria, Kirthevasan Kandasamy, and Barnabás Póczos. A flexible framework for multi-objective bayesian optimization using random scalarizations. In *Uncertainty in Artificial Intelligence*, pages 766–776. PMLR, 2020.
- [39] Victor Picheny. A stepwise uncertainty reduction approach to constrained global optimization. In *Artificial intelligence and statistics*, pages 787–795. PMLR, 2014.
- [40] Victor Picheny. Multiobjective optimization using gaussian process emulators via stepwise uncertainty reduction. *Statistics and Computing*, 25(6):1265–1280, 2015.
- [41] Ali Rahimi and Benjamin Recht. Random features for large-scale kernel machines. *Advances in neural information processing systems*, 20, 2007.
- [42] Dushhyanth Rajaram, Tejas G Puranik, Ashwin Renganathan, Woong Je Sung, Olivia J Pinon-Fischer, Dimitri N Mavris, and Arun Ramamurthy. Deep gaussian process enabled surrogate models for aerodynamic flows. In *AIAA Scitech 2020 Forum*, page 1640, 2020.

-
- [43] C. E. Rasmussen and C. K. I. Williams. *Gaussian Processes for Machine Learning*. MIT Press, 2006.
- [44] Christian P Robert, George Casella, and George Casella. *Monte Carlo statistical methods*, volume 2. Springer, 1999.
- [45] Daniel Russo and Benjamin Van Roy. Learning to optimize via posterior sampling. *Mathematics of Operations Research*, 39(4):1221–1243, 2014.
- [46] Annie Sauer, Robert B Gramacy, and David Higdon. Active learning for deep gaussian process surrogates. *Technometrics*, 65(1):4–18, 2023.
- [47] Bernhard Schölkopf, Alexander Smola, and Klaus-Robert Müller. Nonlinear Component Analysis as a Kernel Eigenvalue Problem. *Neural Computation*, 10(5):1299–1319, July 1998.
- [48] Matthias W Seeger, Christopher KI Williams, and Neil D Lawrence. Fast forward selection to speed up sparse gaussian process regression. In *International Workshop on Artificial Intelligence and Statistics*, pages 254–261. PMLR, 2003.
- [49] Alexander J Smola. Sparse greedy matrix approximation for machine learning. In *Proceedings of the 17th international conference on machine learning, June 29-July 2 2000*. Morgan Kaufmann, 2000.
- [50] Niranjan Srinivas, Andreas Krause, Sham M. Kakade, and Matthias Seeger. Gaussian process optimization in the bandit setting: No regret and experimental design. In *Proceedings of the International Conference on Machine Learning*, 2009.
- [51] Furong Sun, Robert B Gramacy, Benjamin Haaland, Siyuan Lu, and Youngdeok Hwang. Synthesizing simulation and field data of solar irradiance. *Statistical Analysis and Data Mining: The ASA Data Science Journal*, 12(4):311–324, 2019.
- [52] Shinya Suzuki, Shion Takeno, Tomoyuki Tamura, Kazuki Shitara, and Masayuki Karasuyama. Multi-objective bayesian optimization using pareto-frontier entropy. In *International Conference on Machine Learning*, pages 9279–9288. PMLR, 2020.
- [53] Ryoji Tanabe and Hisao Ishibuchi. An easy-to-use real-world multi-objective optimization problem suite. *Applied Soft Computing*, 89:106078, 2020.
- [54] William R Thompson. On the likelihood that one unknown probability exceeds another in view of the evidence of two samples. *Biometrika*, 25(3-4):285–294, 1933.
- [55] Ben Tu, Axel Gandy, Nikolas Kantas, and Behrang Shafei. Joint entropy search for multi-objective bayesian optimization. *Advances in Neural Information Processing Systems*, 35:9922–9938, 2022.
- [56] Zi Wang and Stefanie Jegelka. Max-value entropy search for efficient Bayesian optimization. In *Proceedings of the 34th International Conference on Machine Learning*, volume 70, pages 3627–3635, 2017.
- [57] Christopher Williams and Matthias Seeger. Using the Nyström Method to Speed Up Kernel Machines. In *Advances in Neural Information Processing Systems*, volume 13. MIT Press, 2000.
- [58] Jian Wu and Peter Frazier. The parallel knowledge gradient method for batch Bayesian optimization. In *Advances in Neural Information Processing Systems*, pages 3126–3134, 2016.
- [59] Jian Wu and Peter Frazier. Practical two-step lookahead Bayesian optimization. In *Advances in Neural Information Processing Systems*, pages 9810–9820, 2019.
- [60] Kaifeng Yang, Michael Emmerich, André Deutz, and Thomas Bäck. Efficient computation of expected hypervolume improvement using box decomposition algorithms. *Journal of Global Optimization*, 75:3–34, 2019.
- [61] Kaifeng Yang, Michael Emmerich, André Deutz, and Thomas Bäck. Multi-objective bayesian global optimization using expected hypervolume improvement gradient. *Swarm and evolutionary computation*, 44:945–956, 2019.
- [62] Qingfu Zhang, Wudong Liu, Edward Tsang, and Botond Virginas. Expensive multiobjective optimization by moea/d with gaussian process model. *IEEE Transactions on Evolutionary Computation*, 14(3):456–474, 2009.
- [63] Richard Zhang and Daniel Golovin. Random hypervolume scalarizations for provable multi-objective black box optimization. In *International Conference on Machine Learning*, pages 11096–11105. PMLR, 2020.
- [64] Aimin Zhou, Qingfu Zhang, and Guixu Zhang. A multiobjective evolutionary algorithm based on decomposition and probability model. In *2012 IEEE Congress on Evolutionary Computation*, pages 1–8. IEEE, 2012.
- [65] Eckart Zitzler, Kalyanmoy Deb, and Lothar Thiele. Comparison of multiobjective evolutionary algorithms: Empirical results. *Evolutionary computation*, 8(2):173–195, 2000.

- [66] Marcela Zuluaga, Guillaume Sergent, Andreas Krause, and Markus Püschel. Active learning for multi-objective optimization. In *International Conference on Machine Learning*, pages 462–470. PMLR, 2013.